

ISSN No. 2454-6194 | DOI: 10.51584/IJRIAS | Volume X Issue VI June 2025

Electrical Resistivity Imaging and Lithological Modelling of Hydrocarbon Contaminated Soil in Ogoni, Rivers State, Nigeria

TKS Abam¹, FD Giadom², PM Mogaba³ and IL Nwankwo³

¹Institute of Geosciences and Environmental Management, Rivers State University, Port Harcourt, **Nigeria**

²Department of Geology, University of Port Harcourt, Choba, Port Harcourt, Nigeria

³Groundscan Services Nigeria Limited, Port Harcourt, Nigeria

DOI: https://doi.org/10.51584/IJRIAS.2025.10060005

Received: 05 May 2025; Accepted: 13 May 2025; Published: 27 June 2025

ABSTRACT

Site characterization is critical for effective environmental remediation because it provides the essential data to identify contamination, assess risks, and guide the selection of the most appropriate, cost-effective remediation strategies. A non-intrusive Electrical Resistivity Imaging (ERI) technique was used in combination with intrusive methods to determine the subsoil and groundwater contamination status. The ERI was carried out along a crisscrossing network of VES lines and analyzed using RES2DIV, RES3DIV and Earth-Imager softwares to generate geo-electric tomographs that serve as ground models which are then compared with results of physical assessment of samples from boreholes. Resistivity signature for mature oil contamination was determined and used as cutoff to discriminate between hydrocarbon contamination and other geo-electric horizons. Based on this, contaminated sections of the sub-soil were delineated to define the precise structure and spatial distribution of the contamination zone, as well as determine the volume of soil for remediation. Similarly, lithologic logs derived from borings at the project area were concatenated to produce a 3-dimensional Fence diagram as well as ground model where the contaminated zone could be compared with that generated from the ERI. These ground models are then embedded and overlain on Google Imagery after georectification to relate with ground features and for ease of physical identification on the site. These results suggest that ERI with its minimum footprint and negligible cost can offer substantial benefits in the assessment and delineation of hydrocarbon contaminated zones for effective remediation. Furthermore, the results suggest that the approach can the risk failure of remediation efforts or promote inefficiency, ultimately improving environmental and public health protection.

Keywords: Site Characterization, Electrical Resistivity Imaging, lithological Modelling, Niger Delta

INTRODUCTION

Site characterization is imperative for remediation because it forms the foundation for understanding the nature, extent, and behavior of contamination at a given location. Without an accurate and thorough site assessment, any remedial action may be misdirected, ineffective, or even counterproductive. Site characterization provides the data needed to choose appropriate technologies, estimate costs, evaluate risks, and ensure regulatory compliance.

The over 60 years history of oil exploration in the Niger delta has resulted in several incidents of crude oil spillages (Fig.1) causing soil contamination. These oil spillages may not often be immediately cleaned or remediated due to community claims and agitations. As a result, they remain longer in-situ during which time, they seep into the ground and contaminant soil and groundwater and become concealed from public view in the medium and long-terms.

ISSN No. 2454-6194 | DOI: 10.51584/IJRIAS | Volume X Issue VI June 2025



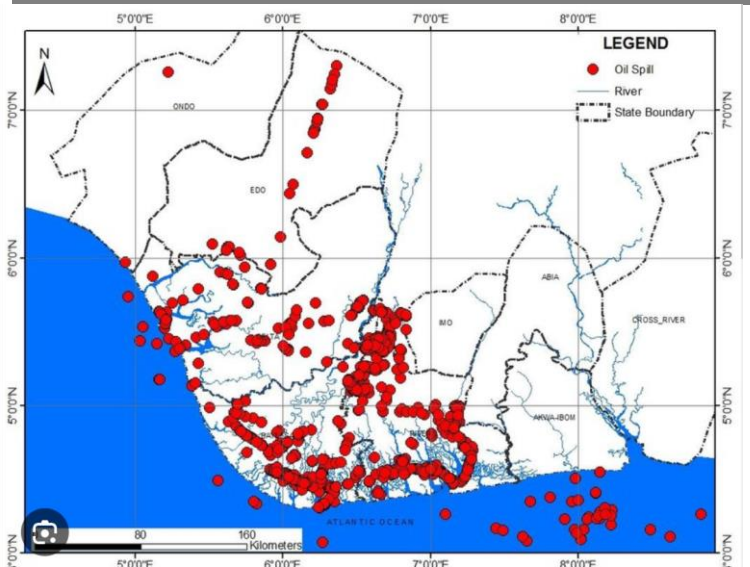


Fig. (1) Spatial distribution of crude oil spillages in the Niger Delta (after Stakeholder Democracy Network 2010)

The traditional approach to soil characterization which relies on intrusive boring degrades the land in addition to increased risks of further contamination. This is apart from being expensive and therefore discouraged from extensive use. Several authors (Olhoeft 1992, Sauck and Mcneil, 1994, Godio and Naldi 2003, Shevnin *et al* 2003, 2006, Arrubarrena-Moreno, Arango-Galván1;2013) have investigated the use and suitability of non-intrusive techniques such as electrical resistivity and ground penetrating radar for detecting crude oil contaminations concealed in the subsoil. The success of these tools depends largely on whether the presence of crude oil and the physical properties that it possesses can be contrasted with those of the host soil. For instance, crude oil contaminated soils do not necessarily produce significant density contrast with the surrounding environment as to promote gravity, seismic techniques or even ground penetrating radar. As a results, these tools or techniques are generally hardly recommended for the characterization of crude oil contaminated sites. Consequently, this paper explores the use of ERI, a non-intrusive technique with minimal footprint and low cost to detect and quantify contaminated area and volumes as well as provide indications of contaminant pathways and receptors.

Electrical Resistivity Imaging relies on the relative ease of electrical current flows through the soil. It has also been shown (Arrubarrena-Moreno and Arango-Galván; 2013) that variations in electrical resistivity (or conductivity) typically correlates with variations in lithology, water saturation, fluid conductivity, porosity and permeability. These properties, when used singly or in combination can be used to map stratigraphic units, geological structure, sinkholes, fractures and groundwater (Shevnin and Delgado, 2002) as well as the low resistivity associated with aged oil-polluted zones (Sauck and McNeil, 1994; Modin et al., 1997; Sauck, 1998, 2000; Atekwana et al., 2001; Abdel-Aal et al., 2001, Omar et al 2006).

It is now widely known that crude oil undergoes degradation after it is spilled on the surface and exposed to the atmosphere, radiation, rainfall and intense or prolonged bacterial action. The degradation of total petroleum hydrocarbons (TPHs) in sand is usually followed by greater microbial mineralization (Qinglong et al (2017). The leachate produced by these chemical reactions between organic acids, CO₂ and mineral grains and grain coatings from an acid environment, created by intense bacterial action on residual hydrocarbons near the base of the vadose zone, according to Sauck (1998), is the source of low resistivity.

Sauck, (1998; 2000) and Atekwana *et al.*, (2001) further explains that the low resistivity zone is developed because of the production of high total dissolved solids in the zone where microbial activity is maximal. Since the production of leachate is dependent on time, it is expected that the resistivity contrast between a hydrocarbon contaminated area and the surrounding rock would depend on the spill age. Thus, low resistivity anomaly is associated with aged crude oil contaminated sites where as in the case of a fresh spill the presence of a high resistive anomaly is expected. Therefore, the age of spill influences the selection and optimization of



ISSN No. 2454-6194 | DOI: 10.51584/IJRIAS | Volume X Issue VI June 2025

the applied technology. ERI reduces the need for extensive drilling, offering a broader spatial coverage and temporal monitoring of contaminant degradation. This is particularly beneficial in assessing the natural attenuation processes of hydrocarbons in the subsurface.

Method of study

The study followed a 2-prong approach using the qualitative, non-intrusive Electrical Resistivity Imaging ERI to predict occurrence of contaminated soil/water and then deploying the quantitative, intrusive boring technique to confirm the prediction of the ERI. The design of the survey lines was informed by understanding of the possible mechanism of contaminant dispersion. In this case, it was understood that the spill emanated from the pipeline and spread on the surface, implying that the topography would provide indication as to the possible directions and trajectory of surface dispersion. This led to a topographic survey which greatly assisted in the construction of a conceptual site model. On the basis of the conceptual site model, and considering the necessity for good spatial coverage, an initial layout of the survey lines was determined.

The acquisition of resistivity data involves the injection of low voltage electric current into the ground via a pair of electrodes and then the resulting potential field is measured by a corresponding pair of potential electrodes. Twenty-six numbers (26 Nos.) Electrical Resistivity Imaging were conducted in the project area to establish the lateral and vertical extent of contamination. The surveyed traverse lines are made to intercept each other as much as possible to enable concatenation of the lines (Fig. 2).

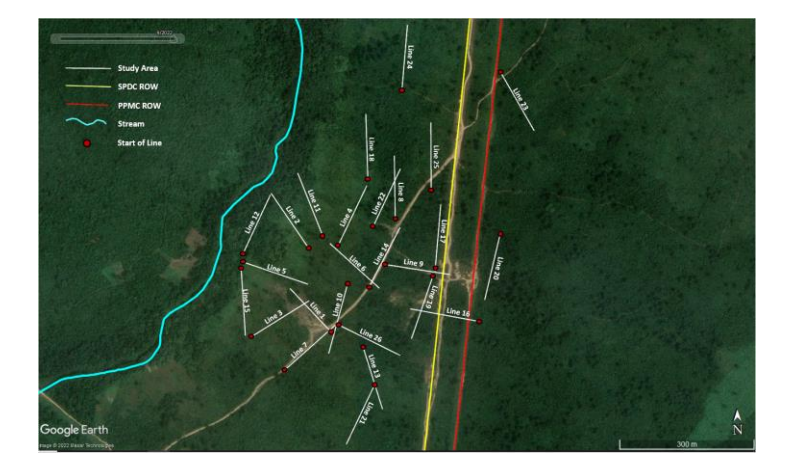


Figure 2: Map showing 2-D ERT survey lines across the project area.

The resistivity survey profiles were typically of 200m in length, using a Wenner electrode configuration. These relatively large number of profiles are necessary since ERI requires a high data density and good coverage of the earth surface for high-resolution images of subsurface targets. The field set-up requires the deployment of an array of regularly spaced electrodes, which are connected to a central control unit via multi-core cables. As a precaution, electrodes are embedded properly since readings can be affected by poor electrical contact at the surface. An increased electrode array length is required to locate deeper depths of interest therefore the site layout must permit long arrays. However, it must be understood that resolution of target features decreases with increased depth of burial.

Resistivity data are then recorded via complex combinations of current and potential electrode pairs to build up a pseudo cross-section of apparent resistivity beneath the survey line. The depth of investigation depends on the electrode separation and geometry, with greater electrode separations yielding bulk resistivity measurements from greater depths. To obtain the best results, the measurements in the field were carried out in a systematic manner so that, as far as possible, all the possible measurements are made to ensure a reliable interpretation. According to Dahlin and Loke (1998) this will enhance the quality of the interpretation model obtained from the inversion of the apparent resistivity measurements. ERI data are rapidly collected with an automated multi-electrode resistivity meter. The recorded data are transferred to a PC for processing. Data processing is based on an iterative routine involving determination of a two-dimensional (2D) simulated model of the subsurface, which is then compared to the observed data and revised (Loke and Barker, 1996).





Convergence between theoretical and observed data is achieved by non-linear least squares optimization. The extent to which the observed and calculated theoretical models agree is an indication of the validity of the true resistivity model (indicated by the final root-mean-squared (RMS) error).

The process of geological noise filtering by the Median algorithm has been described before (Modin et al., 1997; Ritz et al., 1999, Shevnin et al., 2002). This operation is based on characteristics of distortions caused by superficial inhomogeneities. The algorithm was checked and adjusted on modeling and field data and has now about ten years of practical application. In order to derive a cross-sectional model of true ground resistivity, the measured data are subjected to a finite-difference inversion process via RES2DINV (ver 5.1) software. ERI profiles consist of a modeled cross-sectional (2-D) plot of resistivity ($\Omega \cdot m$) versus depth. The true resistivity models are presented as colour contour sections revealing spatial variation in subsurface resistivity. ERI interpretations, supported by borehole data or alternate geophysical data, accurately represent the geometry and lithology of subsurface geologic formations.

Soil Boring, Sampling and Lithological Modelling

Augering complimented by percussion drilling of boreholes to between 7m and 15m below ground level were carried out. Disturbed and undisturbed soil samples were collected at intervals of 0.3m for the first 2m and at 1m interval up to termination of borehole. Groundwater levels were similarly recorded and reduced to datum for computation of groundwater flow direction. Physical observation of hydrocarbon smell and sheen were made on samples at site before transportation to the laboratory for analysis. The locations assessed were georeferenced and incorporated with the results of field activities to produce maps, diagrams, and other technical information useful for characterizing the contaminated area in the assessed site. The soil sampling locations can be plotted and overlain on Google Imagery with an indication of the contamination status. All the drilled boreholes were properly constructed with appropriate well head to restrict unauthorized access as it will be used for contamination monitoring.

Hydrocarbon Contaminant Plume Modelling

The hydrocarbon plume contaminant modelling was carried out using RockWorks. All relevant data for the plume modeling, including contaminant concentrations, lithologic units and well locations were prepared in a compatible format such as spreadsheet or database files and fed into RockWorks. This step involved importing or creating lithology data and interpolating between data points to generate a continuous 3D representation of lithology. A realistic lithologic model is essential for accurate plume modeling. A grid or polygon that encompasses the contaminated area is then created which now defines the area of interest where the plume is present. By associating the concentration values with the corresponding well locations and using RockWorks interpolation tools to estimate contaminant concentrations in areas where data is sparse or missing. An appropriate interpolation method such as inverse distance weighting or kriging is then selected to generate a continuous representation of the contaminant plume. For this project, the kriging interpolation method was utilized. Various visualization tools are then used to display and analyze the plume model. This could be as contour maps, 3D renderings, or cross-sections to visualize the spatial distribution of contaminant concentrations. Red colour was used to represent the contaminated intervals. RockWorks was also used to perform analysis on the plume data, calculate plume volumes, delineate hotspots, and assess the migration direction.

Geology of the project area

The project area is bounded to the east by the Imo River and to the west by a series of creeks. Groundwater occurs in shallow unconfined aquifers consisting of sands and minor clay intercalations. An outline of the geology of the Niger delta (Short and Stauble,1967) highlights several superficial Quaternary sediments in the area of significance to crude oil contamination, including the coastal plain sand, beach ridges, river bars and islands in the mangrove belt, as well as at varying depths in confined aquifers (United Nations Environment Programme, UNEP, 2011). The entire Niger delta region is underlain by three main pervasive geologic Formations in the Niger Delta which comprise from the oldest to youngest as Akata, Agbada and the water bearing multi-aquifer Benin Formation. According to (Etu-Efeotor & Akpokodje, 1990), the upper section of



the Benin Formation (the quaternary deposits which host the hydrocarbon contaminants) is about 40 - 150 m thick and comprises sand and silt/clay with the later becoming increasingly more prominent seawards.

RESULTS AND DISCUSSION

Field Assessment began with topographic surveys of the surrounding area (Fig. 3) to determine the possible surface runoff directions and risk levels of potential accumulation of surface derived hydrocarbon pollution. Fig.3 indicates that the central area within the 18m contour envelop is low lying and could serve as a zone of potential accumulation of surface runoff.

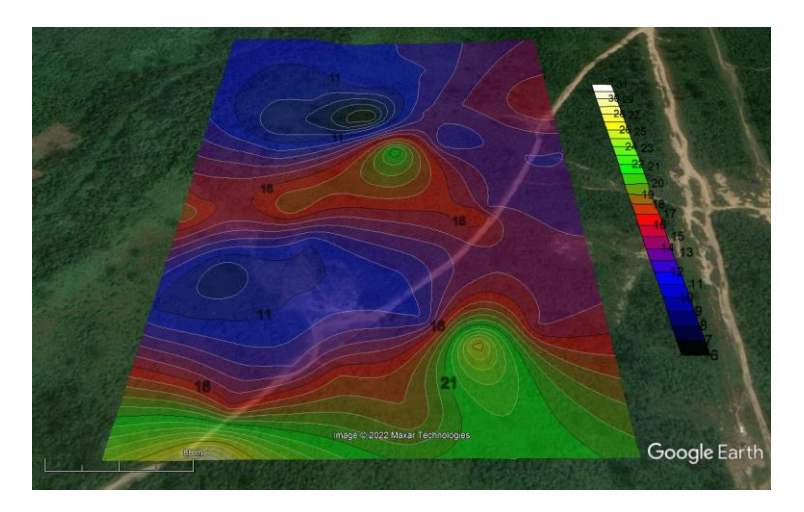


Figure 3: Topography of the Oka Nsinmu Ogale Area with possible hydrocarbon pollution

Non-intrusive Electrical Resistivity Imaging (ERI)

The results of pseudo section and tomographs based on the electrical resistivity are selectively presented as vertical apparent resistivity cross-sections along profiles. Due to limited space, only four of the twenty-six profile lines spread across the project area have been presented to illustrate the occurrence of contamination and the interpretation of the tomographs. All imaging is performed after removing the geological noise.

Figures (4 to 7) are vertical cross-section of apparent resistivity for soundings along selected profiles and interpreted using RES2DINV and Earth-Imager softwares respectively to see how both output compare.

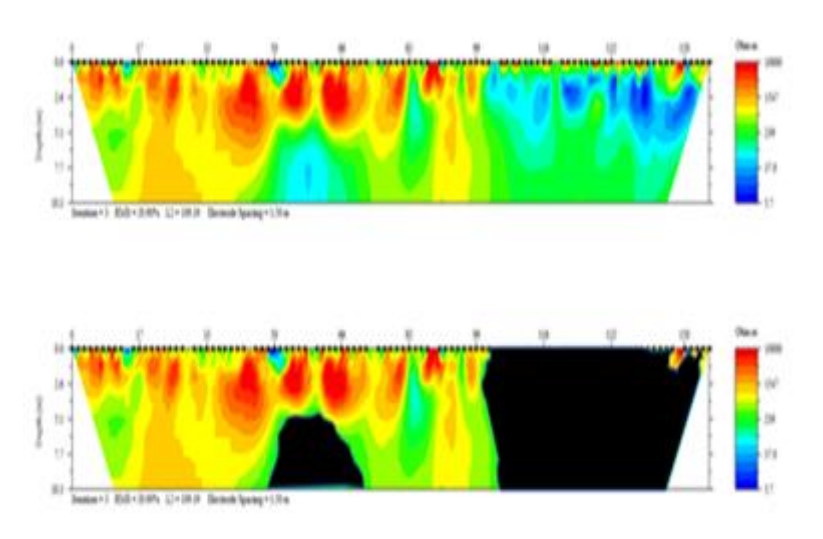


Figure 4: Processed electrical resistivity tomogram for Line 3 using Earth-Imager software (dark area highlighted on second tomogram shows oil contaminated zones with resistivity values $\leq 550 \Omega m$)

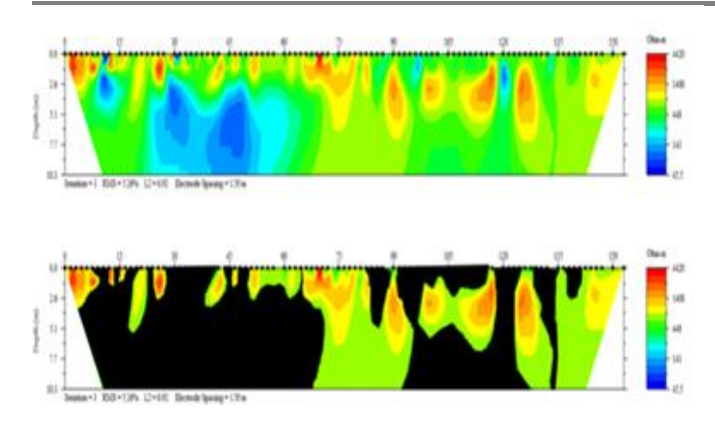


Figure 5: Processed electrical resistivity tomogram for Line 11 using Earth-Imager software (dark area highlighted on second tomogram shows oil contaminated zones with resistivity values \leq 550 Ω m)

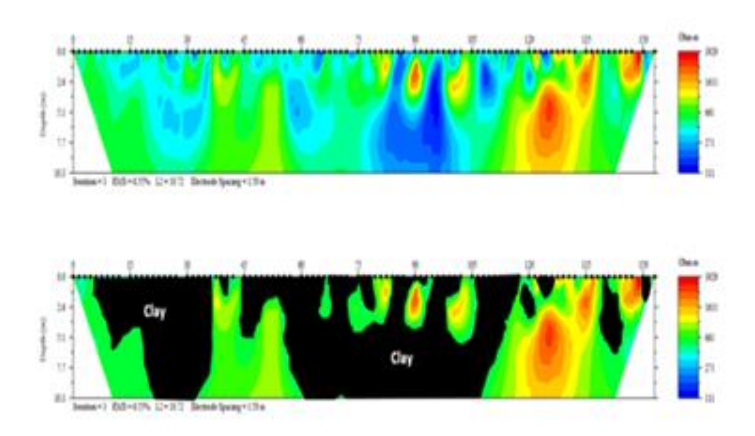


Figure 6: Processed electrical resistivity tomogram for Line 12 using Earth-Imager software (dark area highlighted on second tomogram shows the presence of thick clays)

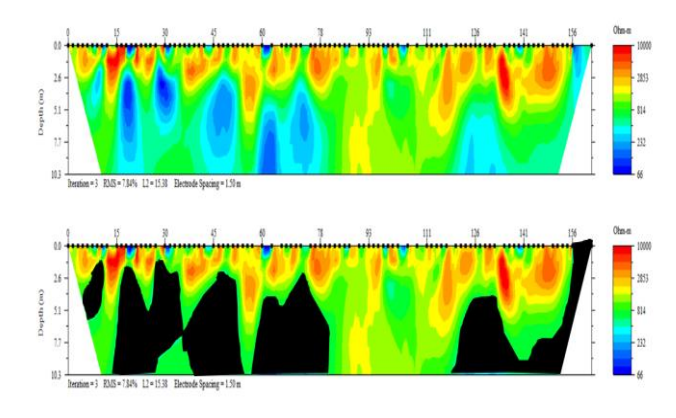


Fig.7: Processed electrical resistivity tomogram for Line 25 using Earth-Imager software (dark area highlighted on second tomogram shows oil contaminated zones with resistivity values \leq 550 Ω m)

Line 3 lies 300m west of the Pipeline Right of Way (PPROW) and trends in the NE-SW direction with a total line length of 150.0m (Fig. 4). Along this line, a major oil plume was found from 99 m to 150 m on the ground surface and extended through the maximum investigation depth of 10.10 m. A smaller deep-seated plume was found between 48 and 72 m on the surface, and from 8.50 m depth to 10.1m depth.

Line 11 lies 300m west of the PPROW and trends in the NW-SE direction with a total line length of 150.0m (Fig. 5). Along this line, two oil plumes were found between 0.0 m to 72.0 m and between 108 m to 150 m on the ground surface which extended from the surface through the maximum investigation depth of 10.10 m. Some small uncontaminated sections were found dispersed within the shallow area.

Line 12 lies 400m west of the PPROW and trends in the NNE-SSW direction with a total line length of 150.0m (Fig. 6). This line lies 10 m away and parallel to the bank of a stream channel. Along this line, areas with low resistivity signatures were indicative of thick clays. The low resistivity values coincided with very low induced polarization measurements which ranged between 0.36 ms to 1.49 ms. Low resistivity signatures coinciding with low IP measurements are indicative of clayey soil (Deceuster and Kaufmann, 2012). Soil augering was used to validate the presence of clays at this location.

Line 25 lies 50 m west of the PPROW and trends in the N-S direction with a total line length of 150.0m (Fig. 7). Along this line, two major oil plumes were found between 0.0 m and 75.0m and between 120 m and 150 m on the ground surface. The plumes extended from a shallow depth of 2.0 m to the maximum investigation depth of 10.10 m.

Tomographs of the 26 profiles lines with start and end point coordinates are concatenated to produce 3-D resistivity inversion grid showing (Fig.8) ground resistivity distribution.

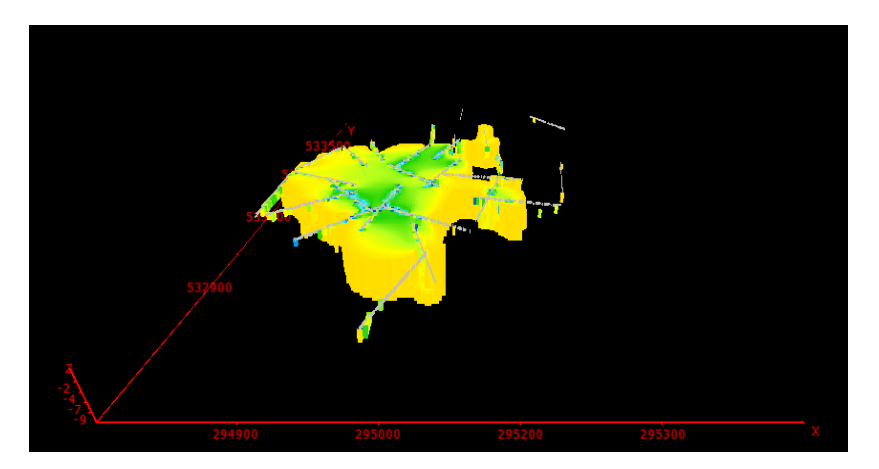


Figure 8: 3-D resistivity inversion grid generated in Res3DINV software after applying a cut-off value 550 Ohm.m

Resistivity tomogram display based on Earth Imager for 3.0m depth overlaid on google map after applying a resistivity cut-off for oil contamination at \leq 550 Ohm.m) is presented in Fig. 9. There were fears that a nearby freshwater stream which was a potential receptor would be impacted. Based on the tomography using Earth Imager, this was not to be so due to the presence of a clay liner (which extended beyond 3m) preventing further northwest migration in addition to southeast oriented groundwater flow direction (Fig. 9). Looking further at the flow direction of the groundwater, it would appear that the creek is a source of recharge for the groundwater.

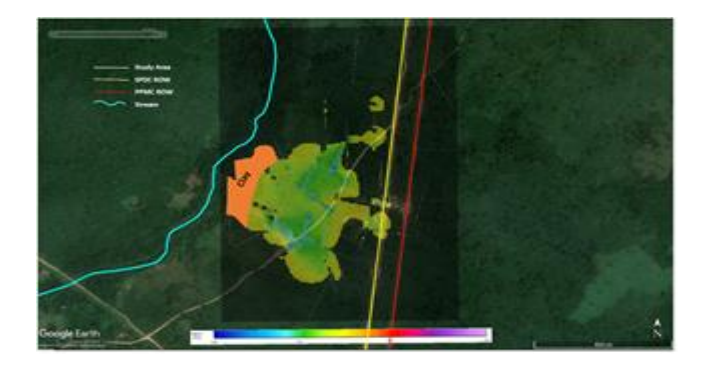


Fig. 9: Resistivity tomogram for 3.0m depth

Delineation of the Area Contaminated by Hydrocarbon

The delineated contamination was estimated from calculating the area covered by the contaminated soil and groundwater which is a KML shape file type displayed as polygon of known area, perimeter, centroid, and bounding box amounting to 119,565m² (Fig 10). The results highlight the shape of the plume and also reveals the extent of contamination and area requiring active remediation. This strongly suggests that resistivity as a tool for characterization should not be employed as a stand-alone tool but borehole data should be used as a form of calibration to help constrain resistivity models in order to get more improved interpretations. The contaminated area in Figure 10 below was estimated to be approximately 119,565m².

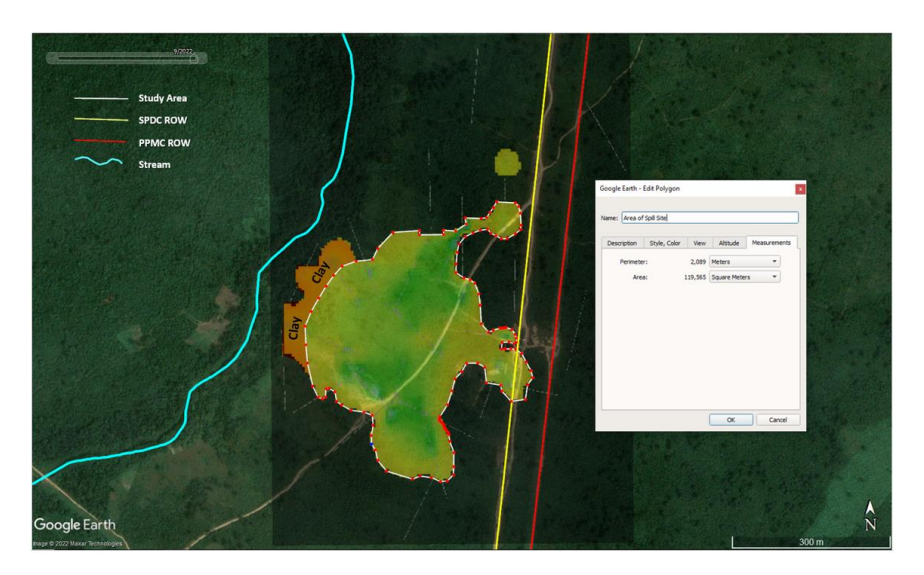


Figure 10: Hydrocarbon contaminated delineated area based on resistivity data. The total surface area delineated is 119,565m²

Lithologic Modelling and Oil Contamination Volume Estimated for Oka Nsimu Community

The lithologic logs from auger and percussion borings and the status of contamination (Fig. 11) were combined to produce a 3-dimensional Fence diagram. The contaminated horizons were then extracted as shown in Fig. (12) and subsequently overlain on Google Imagery to relate ground features and for ease of physical identification.

Depth																					
(m)	DESCRIPTION	STRATA	WL	20	21	22	23	24	25	26	27	28	29	30	31	32	33	34	35	36	37
	Dark brown silty			NO	NO HC	NO HC	NO HC	NO HC	NO HC	NO HC	NO HC	NO HC	NO HC	NO HC	NO HC	NO HC	NO HC	NO HC	NO HC	NO	NO HC
0.3	sand			HC	Smell &	Smell &	Smell &	Smell &	Smell &	Smell &	Smell &	Smell &	Smell &	Smell &	Smell &	Smell &	Smell &	Smell &	Smell &	HC	Smell
				NO	NO HC	NO HC	NO HC	Low HC	Low HC	NO HC	NO HC	NO HC	NO HC	NO HC	NO HC	NO HC	NO HC	NO HC	NO HC	NO	NO HC
1	Brownish silty sand			HC	Smell &	Smell &	Smell &	smell &	smell &	Smell &	Smell &	Smell &	Smell &	Smell &	Smell &	Smell &	Smell &	Smell &	Smell &	HC	Smell
	Brownish grey silty			Stron	NO HC	NO HC	NO HC	Mild HC	Strong HC	NO HC	Strong HC	NO HC	NO HC	NO HC	NO HC	Low HC	NO HC	NO HC	NO HC	NO	NO HC
2	sand			g HC	Smell &	Smell &	Smell &	smell &	smell &	Smell &	smell &	Smell &	Smell &	Smell &	Smell &	smell &	Smell &	Smell &	Smell &	HC	Smell
	Brownish grey coarse			Stron	Mild HC	Strong	NO HC	Strong HC	Strong HC	NO HC	Strong HC	Low HC	NO HC	NO HC	Mild HC	Strong	Strong	Mild	NO HC	NO	Mild
3	clayey soil		3.6n	g HC	smell &	HC smell	Smell &	smell &	smell &	Smell &	smell &	smell &	Smell &	Smell &	smell &	НС	HC	НС	Smell &	HC	HC
				Stron	Strong	Strong	Strong	Strong HC	Strong HC	Strong HC	Strong HC	Low HC	NO HC	NO HC	Mild HC	Mild HC	Strong	Strong	Strong	NO	Strong
4	Grey silty clay			g HC	HC smell	HC smell	HC smell	smell &	smell &	smell &	smell &	smell &	Smell &	Smell &	smell &	smell &	HC	HC	HC	HC	HC
				Stron	Strong	Strong	Strong	Strong HC	Strong HC	Strong HC	Strong HC	Low HC	NO HC	NO HC	Mild HC	Mild HC	Strong	Strong	Strong	Low	Strong
5	Grey silty sand			g HC	HC smell	HC smell	HC smell	smell &	smell &	smell &	smell &	smell &	Smell &	Smell &	smell &	smell &	HC	HC	HC	HC	HC
				Stron	Strong	Strong		Strong HC	Low HC	Strong HC	Strong HC	NO HC	NO HC	NO HC	Mild HC	Low HC	Strong	Strong	Strong		Strong
6	Grey silty sand			g HC	HC smell	HC smell		smell &	smell &	smell &	smell &	Smell &	Smell &	Smell &	smell &	smell &	HC	HC	HC		HC
				Mild	NO HC			Strong HC	NO HC		Strong HC	NO HC	NO HC	NO HC	Mild HC	Low HC		Strong			Strong
7	Ash Grey silty sand			НС	Smell &			smell &	Smell &		smell &	Smell &	Smell &	Smell &	smell &	smell &		HC			HC
				Mild								NO HC		NO HC		Low HC					Strong
8	Grey coarse sand			НС								Smell &		Smell &		smell &					HC

Fig.11: Lithologic units and state of contamination observed in some of the boreholes within the project area

ISSN No. 2454-6194 | DOI: 10.51584/IJRIAS | Volume X Issue VI June 2025

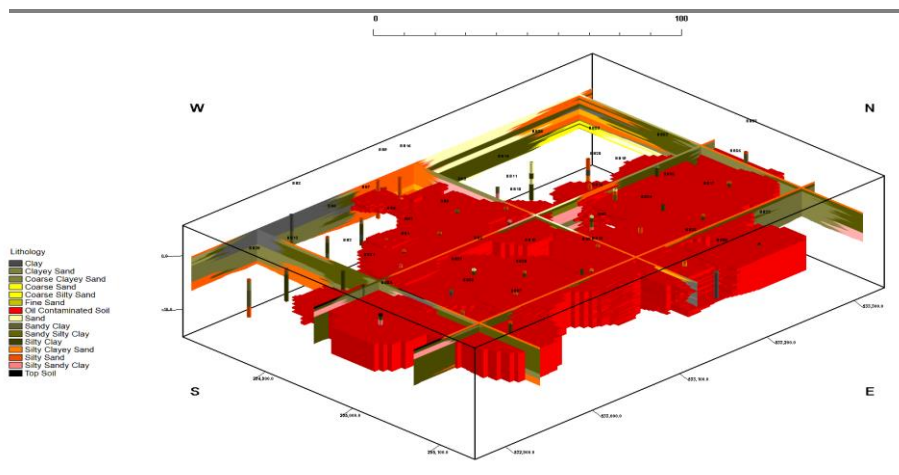


Figure 12: A 3-D fence diagram showing the lithologic units encountered within the project area

Using this, the hydrocarbon contaminated area was computed as 102,596m². while the volume of contaminated soil materials was calculated as 429,020m³.

CONCLUSION AND RECOMMENDATION

This study has demonstrated that ERI is a reliable and effective tool in the identification and delineation of contaminated zones. The comparison between the results of ERI and lithological modeling of the hydrocarbon concentrated soil is a confirmation that ERI can provide detailed insights into subsurface structures and contaminant distributions and allows for improved characterization of contamination zones, which is crucial for effective remediation strategies.

Repetition of the characterization process with time intervals has the potential to monitor changes at a contaminated site and determine the effectiveness of an eventual remediation process. Presentation of delineated contaminated areas in 3-D models overlain on Google Imagery facilitates has improved the visualization and identification of impacted areas and boundaries.

It is recommended that the use of ERI be given an increased attention since it is a low-cost and high-resolution technique that can rapidly image states and processes. While ERI offers substantial benefits, it is essential to recognize that improper application or misinterpretation of data can lead to inaccuracies in lithological modeling, emphasizing the need for careful implementation and validation of results.

REFERENCES

- 1. Abdel-Aal, G. Z., D. D. Werkema, W. A. Sauck JR. and E. Atekwana, (2001). Geophysical investigation of vadose zone conductivity anomalies at a former refinery site, Kalamazoo, MI. In: Proceedings of the Symposium on the Application of Geophysics to Engineering and Environmental Problems, 1–9
- 2. Atekwana, E., D. P. Cassidy, C. Magnuson, A. L. Endres, D. D. Werkema, JR. and W. A. Sauck, (2001). Changes in geoelectrical properties accompanying microbial degradation of LNAPL. In: Proceedings of the Symposium on the Application of Geophysics to Engineering and Environmental Problems, 1–10.
- 3. Bailey, N. J. L., H. R. Krouse, C. R. Evans and M. A. Rogers, (1973). Alteration of Crude Oil by Waters and Bacteria Evidence from Geochemical and Isotope Studies. Am. Assoc. Petrol. Geol. Bull., 57, 1276–1290.
- 4. Blome, M., Maurer, H. and Schmidt, K. (2009), Advances in three-dimensional geoelectric forward solver techniques. Geophys. J. Int. 176: 740-752, 2009.
- 5. Blome, M., Maurer, H. and Greenhalgh, S., Geoelectric experimental design Efficient acquisition and exploitation of complete pole-bipole data sets. Geophysics 76: F15-F26, 2011.



ISSN No. 2454-6194 | DOI: 10.51584/IJRIAS | Volume X Issue VI June 2025

- 6. Dahlin, T. and Loke, M. (1998) Resolution of 2-D Resistivity Imaging Wenner as Assessed by Numerical Modeling. Journal of Applied Geophysics, 38, 237-249. https://doi.org/10.1016/S0926-9851(97)00030-X
- 7. Etu-Efeotor, J.O., and Akpokodje E.G. (1990). Aquifer systems of the Niger Delta. Journal of Minning Geology, 26(2), 279-285.
- 8. Godio, A., Naldi, M., (2003), Two-dimensional electrical imaging for detection of hydrocarbon contaminants: Near Surface Geophysics, 1, 131-137.
- 9. Gunther, T., Rucker, C. and Spitzer, K., (2006) 3-d modeling and inversion of DC resistivity data incorporating topography Part II: Inversion. Geophys. J. Int. 166: 506-517, 2006.
- 10. Keller, G. and F. Frischknecht, (1966). Electrical Methods in Geophysical Prospecting. MODIN, I. N., V. A. SHEVNIN et al., 1997. Investigations of oil pollution with electrical prospecting methods. In: Proceedings of the 3rd EEGS-ES Meeting. Aarhus, Denmark, 8-11 September 1997, 267-270.
- 11. LaBrecque, D. J., Miletto, M, Daily, W., Ramirez, A. and Owen, E.,(1996) The effects of noise on Occam's inversion of resistivity tomography data, Geophysics 61; 538? 548, 1996.
- 12. LaBrecque, D. J., and Yang, X., Difference Inversion of ERT Data: a Fast Inversion Method for 3-D in Situ Monitoring: J. Environ. Eng. Geophys. 6: 83, 2001.
- Loke, M.H., (2010), Tutorial, 2D and 3D electrical imaging surveys: available on http://www.landvizer.biz/forall/RES2DINV/CourseNotes.pdf
- 14. Loke, M.H., Barker, R.D., (1996), Rapid least-squares inversion of apparent resistivity pseudosections using a quasi-Newton method: Geophysical Prospecting, 44, 131-152.
- 15. Arrubarrena-Moreno M, Claudia Arango-Galván (2013) Use of electrical resistivity tomography in the study of soil pollution caused by hydrocarbons: Case study in Puebla (México) Boletín de la Sociedad Geológica Mexicana Volumen 65, núm. 2, 2013, p. 419-426
- 16. Nash, M. S., E. Atekwana and W. A. Sauck, (1997). Geophysical investigation of anomalous conductivity at a hydrocarbon contamination site. In: Proceedings of the Symposium on the Application of Geophysics to Engineering and Environmental Problems, 675-683
- 17. NOSDRA (2022) Nigerian Oil Spill Monitor 2022 Edition. https://nosdra.oilspillmonitor.ng/
- 18. Olhoeft, G. R., (1992). Geophysical detection of hydrocarbon and organic chemical contamination. In: Proceedings of the Symposium on the Application of Geophysics to Engineering and Environmental Problems, 587-595.
- 19. Omar Delgado-Rodríguez, Vladimir Shevnin1, Jesús Ochoa-Valdés and Albert Ryjov (2006) Geoelectrical characterization of a site with hydrocarbon contamination caused by pipeline leakage, Geofísica Internacional, Vol. 45, Num. 1, pp. 63-72
- 20. Qinglong Liu, Jingchun Tang, Kai Gao, Ranjit Gurav and John P. Giesy (2017) Aerobic degradation of crude oil by microorganisms in soils from four geographic regions of China. Sci Rep. 2017; 7: 14856. Published online 2017 Nov 1. doi: 10.1038/s41598-017-14032-5
- 21. Ritz, M., H. Robain, E. Pervago, Y. Albouy, CH. Camerlynck, M. Descloitres and A. Mariko, (1999). A. Improvement to resistivity pseudosection modeling by removal of near-surface inhomogeneity effects: application to a soil system in south Cameroon". Geophys. Prospect., 47, 85–101.
- 22. Rucker, C., Gunther, T. and Spitzer, K., 3-d modeling and inversion of DC resistivity data incorporating tomography Part II: Inversion. Geophys. J. Int. 166: 495-505, 2006.
- 23. Sauck, W. A. and J. Mcneil, (1994). Some problems associated with GPR detection of hydrocarbon plumes; Fifth International Conference on Ground Penetrating Radar (GPR'94).
- 24. Sauck, W. A., (1998). A conceptual model for the geoelectrical response of LNAPL plumes in granular sediments. In: Proceedings of the Symposium on the Application of Geophysics to Engineering and Environmental Problems, 805-817.
- 25. Sauck, W. A. (2000). A Model for the Resistivity Structure of LNAPL Plumes and Their Environs in Sandy Sediments. Journal of Applied Geophysics, 44, 151-165. https://doi.org/10.1016/S0926-9851(99)00021-X
- 26. Shevnin, V., A. Ryjov, E. Nakamura, A. Sánchez, V. Korolev and A. Mousatov, 2002. Study of oil pollution in Mexico with resistivity sounding. In: Proceedings of the Symposium on the Application of Geophysics to Engineering and Environmental Problems.

INTERNATIONAL JOURN

INTERNATIONAL JOURNAL OF RESEARCH AND INNOVATION IN APPLIED SCIENCE (IJRIAS)

ISSN No. 2454-6194 | DOI: 10.51584/IJRIAS | Volume X Issue VI June 2025

- 27. Shevnin, V. and O. Delgado, (2002). Application of resistivity sounding method for oil pollution study in urban and rural areas. In: Proceedings of the Symposium on the Application of Geophysics to Engineering and Environmental Problems.
- 28. Shevnin, V., Delgado-Rodríguez, O., Fernández-Linares, L., Zegarra- Martínez, H., Mousatov, A., Ryjov, A., (2005), Geoelectrical Characterization of an oil-contaminated site in Tabasco, Mexico: Geofísica Internacional, 44, 251-263.
- 29. Shevnin, V., Delgado-Rodríguez, O., Mousatov, A., Flores-Hernández, D., Zegarra-Martínez, H., Ryjov, A., (2006), Estimation of soil petrophysical parameters from resistivity data: Application to oil-contaminated site characterization: Geofísica Internacional, 45, 179-193.
- 30. Short, K. C., and Stauble A. J (1967). Outline geology of the Niger Delta. American Association of Petroleum Geologists Bulletin, 54, 761-779.
- 31. Vladimir Shevnin, Omar Delgado-Rodríguez, Aleksandr Mousatov, Edgar Nakamura-Labastida and Abraham Mejía-Aguilar (2003) Oil pollution detection using resistivity sounding. Geofísica Internacional (2003), Vol. 42, Num. 4, pp. 613-622